European Journal of Nuclear Medicine and Molecular Imaging
https://doi.org/10.1007/s00259-018-3989-0

ORIGINAL ARTICLE

^{18}F-PSMA-1007 PET/CT at 60 and 120 minutes in patients with prostate cancer: biodistribution, tumour detection and activity kinetics

Kambiz Rahbar[1] · Ali Afshar-Oromieh[2] · Martin Bögemann[3] · Stefan Wagner[1] · Michael Schäfers[1] · Lars Stegger[1] · Matthias Weckesser[1]

Received: 31 January 2018 / Accepted: 28 February 2018
© Springer-Verlag GmbH Germany, part of Springer Nature 2018

Abstract

Purpose PSMA-targeted PET in patients with prostate cancer (PCa) has a significant impact on treatment decisions. By far the most frequently used PSMA ligand is ^{68}Ga-labelled PSMA-11. However, due to the availability of larger amounts of activity, ^{18}F-labelled PSMA ligands are of major interest. The aim of the present study was to evaluate the biodistribution and performance of the novel ^{18}F-labelled ligand PSMA-1007 at two different time points.

Methods This retrospective analysis included 40 consecutive patients (mean age 68.7 ± 8.1 years) referred for PSMA PET/CT. ^{18}F-PSMA-1007 PET/CT was performed for localization of biochemical relapse, primary staging or therapy follow-up. Circular regions of interest were placed on representative slices of the liver, spleen, kidney, abdominal aortic blood pool, bone marrow (fourth lumbar vertebral body), urinary bladder and gluteus muscle at 60 and 120 min after injection. In malignant lesions the maximum standardized uptake (SUV_{max}) was measured within volumes of interest at both time points. All SUVs at 60 min were compared with those at 120 min after injection.

Results The activity in the blood pool, urinary bladder and gluteus muscle was very low and decreased significantly over time ($P < 0.001$). Uptake in the liver, spleen and kidney showed a significant increase over time and uptake in the bone marrow remained stable. Overall, 135 PCa lesions were detected at 60 min and 136 lesions at 120 min after injection. The median SUV_{max} increased significantly ($P < 0.001$) from 10.98 to 15.51 between 60 and 120 min.

Conclusion PCa lesions show a significant increase in ^{18}F-PSMA-1007 uptake at 120 min compared with 60 min after injection. In addition, accumulation of the tracer in the urinary bladder was very low leading to improved contrast of adjacent PCa lesions. Increasing accumulation in the liver may limit the sensitivity of the tracer in detecting liver metastases.

Keywords Prostate cancer · PSMA-1007 · PET/CT

Introduction

Prostate cancer (PCa) is the most common cancer in men [1]. Therefore, diagnostic strategies are of great economic and medical interest. Within the last decade several diagnostic tools have been developed and implemented in the management of patients with PCa. In this context, prostate-specific membrane antigen (PSMA) has received increasing attention as an excellent target for imaging and therapy of PCa. PSMA, also known as glutamate carboxypeptidase II, *N*-acetyl-α-linked acidic dipeptidase I or folate hydrolase, is a type II transmembrane glycoprotein, which is strongly overexpressed in PCa cells. The level of PSMA expression increases with increasing tumour dedifferentiation and in metastatic and hormone-refractory cancers [2–4]. Despite its name, PSMA is not specific to PCa. Several other organs and tumour entities show PSMA expression, although usually at a lower level than PCa [5, 6]. Amongst these tissues are the kidneys, lacrimal and salivary glands, parts of the small and large intestines, liver, spleen, neuronal ganglia, and various solid malignant and benign tumours, and PSMA is also expressed in inflammatory processes [5–7].

✉ Kambiz Rahbar
rahbar@uni–muenster.de

[1] Department of Nuclear Medicine, University Hospital Münster, Albert-Schweitzer-Campus 1, 48149 Münster, Germany

[2] Department of Nuclear Medicine, Inselspital, University Hospital Bern, Bern, Switzerland

[3] Department of Urology, University Hospital Münster, Münster, Germany

Published online: 14 March 2018

Following many years of outstanding preclinical research, the clinical breakthrough in PSMA-based imaging was achieved with the introduction of ^{68}Ga-PSMA-11 in May 2011 as a PET tracer. Since then, this novel method of imaging has rapidly spread worldwide and is regarded as a significant step forward in the management of PCa [5, 8–11]. The main reasons for the rapid spread of this method are the characteristics of ^{68}Ga-PSMA-11 that include its excellent tumour uptake, low background signal, high specificity and very fast pharmacokinetics that result in superior tumour visibility compared with other methods [12]. However, ^{18}F shows advantages over ^{68}Ga including the larger amount of activity from fluorine-18 production by cyclotron compared with the limited activity of gallium-68 derived from elution of ^{68}Ge/^{68}Ga generators, the longer half-life and the higher physical spatial resolution. In recent years several ^{18}F-labelled ligands have been introduced by different groups: DCFBC [13], DCFPyL [14], and PSMA-1007 [15]. The aims of the present study were to evaluate the performance of ^{18}F-PSMA-1007 and to analyse its biodistribution at two different time points.

Materials and methods

From October 2017, 40 consecutive patients who were referred for PSMA PET/CT were included in this retrospective analysis. ^{18}F-PSMA-1007 PET/CT was performed for localization of biochemical relapse, primary staging or therapy follow-up. All patients received detailed information about the imaging procedures and provided signed informed consent according institutional guidelines. Of the 40 patients, 28 presented with biochemical relapse after primary therapy, 9 were scanned for therapy follow-up and 3 were scanned for primary staging to rule out distant metastasis prior to radical prostatectomy.

Imaging procedures and preparation of ^{18}F-PSMA-1007

^{18}F-PSMA-1007 was produced in a GE TracerLab MX synthesizer according to the one-step procedure described by Cardinale et al. [16] including sterile filtration of the final batch solution. ^{18}F-PSMA-1007 precursor, cassettes and reagents for the synthesis of ^{18}F-PSMA-1007, as well as the synthesis sequence for full-automatic production with a GE TracerLab MX module were obtained from ABX advanced biochemical compounds GmbH (Radeberg, Germany). The final injection solution of the ^{18}F-PSMA-1007 batch was clear, colourless and particle-free, and had a mean radiochemical purity of 96.5 ± 1.1% (range 95–99%) determined by high-performance liquid chromatography. Unreacted ^{18}F-fluoride or ^{18}F-fluoride resulting from compound cleavage was not detected by thin-layer chromatography. The pH of the batch solution ranged from 5.9 to 7.8 and the endotoxin content was <5.0 Endotoxin Units/ml. Ethanol and dimethyl sulphoxide (DMSO) were measured as residual solvents by gas chromatography and the concentrations were determined (ethanol 29.6–31.6 mg/ml; DMSO 0.25–0.68 mg/ml). Moreover, the osmolality ranged from 1,110 to 1,300 mOsmol/kg.

Patients received 4 MBq per kg body weight with a maximum of 400 MBq per patient (mean injected activity 336.7 ± 46 MBq). The first scan was performed 60 min after injection starting at the inguinal region with three bed positions including the liver. The second scan was performed 120 min after injection starting at the lower limbs to the skull (Fig. 1). Patients were asked to void their bladder before each scan. Images were acquired with a scan time of 3 min per bed position on a Siemens mCT scanner (Siemens Healthcare). Images were reconstructed using standard software supplied by the manufacturer. For attenuation correction, a low-dose CT scan was performed corresponding to the PET acquisition. A contrast-enhanced CT scan of the abdomen and pelvis was only performed if no imaging was performed before the PET scan.

Image analysis

Analysis was performed on coregistered images using the *syngo*.via software (version VB20A; Siemens Healthcare).

Fig. 1 Maximum intensity projection of ^{18}F-PSMA-1007 PET images obtained at 60 and 120 min after injection showing the distribution of ^{18}F-PSMA-1007 in normal organs

Activity (mean standardized uptake value, SUV_{mean}) in normal tissue was measured in the blood pool, liver, spleen, kidney, urinary bladder, gluteus muscle and bone/bone marrow. Blood-pool activity was measured in the abdominal aorta. Bone/bone marrow activity was measured in the fourth lumbar vertebral body at both imaging time points. Circular regions of interest were placed on representative slices of the liver, spleen, kidney, abdominal aortic blood pool, bone marrow (fourth lumbar vertebral body), urinary bladder and gluteus muscle. Normal uptake of ^{18}F-PSMA-1007 (SUV_{mean}) in the above-mentioned organs/tissues were analysed quantitatively in all patients (Table 2).

In malignant lesions volumes of interest were placed on the plane with the highest uptake, and the maximum standardized uptake (SUV_{max}) was measured. Any visible PCa lesions in patients were analysed unless they had more than five lesions in the same compartment, in which case a maximum of five randomly selected lesions were analysed. This selection strategy avoided overestimation of SUVs in the patient cohort as otherwise dominant lesions would have been preferentially selected.

Statistical analysis

SPSS Statistics 25 (IBM Inc. Armonk, NY, USA) was used for statistical analysis. Descriptive statistics are absolute and relative frequencies, means or medians and standard deviations or ranges were used to characterize the study population. Wilcoxon's signed-ranks test was used to analyse the significance of differences in median SUV_{max} and SUV_{mean} between 60 and 120 min after injection. To compensate for the use of multiple testing, only P values <0.01 were accepted as significant.

Results

This retrospective analysis included 40 patients (mean age 68.7 ± 8.1 years) of whom 28 had a biochemical relapse after primary therapy, 9 were scanned for therapy follow-up and 3 were scanned for primary staging to rule out distant metastasis prior to radical prostatectomy. Patient characteristics at baseline are given in Table 1.

Image analysis

^{18}F-PSMA-1007 activity in the blood pool, urinary bladder and gluteus muscle decreased significantly over time ($P < 0.001$, Table 2). Uptake in the liver, spleen and kidney showed a significant increase over time and uptake in the bone marrow remained stable (Table 2).

In 38 patients (95%), at least one lesion attributable to PCa was detected. In two patients scanned to localize biochemical relapse, no enhanced ^{18}F-PSMA-1007 uptake was detected. PSA values in these two patients were 0.41 and 0.88 ng/ml. In six of eight patients (75%) with a PSA value <1 ng/ml and in all patients with a PSA value ≥1 ng/ml the scan was pathological. Table 2 shows the SUV_{max} of all lesions characteristic of PCa. Overall, 136 lesions were detected at both time points with a significant increase in median SUV_{max} from 10.98 to 15.51 ($P < 0.001$, Table 2). The increase was significant for primary tumours, lymph nodes and skeletal metastases (Table 2). All lesions were visible at both time points, with the exception of one lymph node which was visible at 120 min only (Fig. 2). In four lesions characteristic of PCa (two bone lesions and two lymph nodes) SUV_{max} decreased slightly from the first to the second time point.

Table 1 Characteristics of the 40 patients included

Characteristic	n
Age (years), mean ± SD	68.7 ± 8.1
PSA value (ng/ml), mean (range)	35.4 (0.03–939)
Gleason score, *n*	
7	8
8	6
9	9
10	1
Unknown	16
Previous therapy, *n*	
Prostatectomy	31
External irradiation	16
Antihormonal therapy	14
Chemotherapy	6
Abiraterone	6
Enzalutamide	1
PSMA radioligand therapy	3
Radium-223	1

PSA prostate-specific antigen, *PSMA* prostate-specific membrane antigen

Discussion

The present study evaluated the uptake of ^{18}F-PSMA-1007 in PCa lesions and in normal organs at 60 and 120 min after injection. In normal organs, an increase in ^{18}F-PSMA-1007 uptake was seen in the liver, spleen and kidneys, whereas uptake in the urinary bladder, blood pool and gluteus muscle decreased significantly. The decrease in ^{18}F-PSMA-1007 uptake in the blood pool and gluteal muscle over time is in line with published data on PSMA ligands [5, 17]. The activity measured in the urinary bladder was very low at 60 min after injection and also decreased significantly over time (Fig. 3). The images suggest early renal elimination, but in late images there was nearly no activity in the urinary bladder and no

Table 2 Comparison of ^{18}F-PSMA-1007 uptake 60 and 120 min after injection in different tissues

Tissue	No. of lesions	Acquisition time (minutes after injection)	Median SUV_{max}	Median SUV_{mean}	Interquartile range	*P* value[a]
Malignant						
All lesions	136	60	10.98		5.97–25.18	<0.001
		120	15.51		8.29–31.85	
Prostate	17	60	9.78		5.22–22.71	<0.001
		120	15.02		7.13–32.99	
Lymph nodes	73	60	10.96		5.08–27.52	<0.001
		120	15.80		6.47–37.93	
Bone	46	60	12.62		7.02–24.41	<0.001
		120	15.11		9.72–31.67	
Normal						
Liver	40	60		9.69	8.11–12.23	<0.001
		120		12.04	10.58–14.13	
Spleen	40	60		9.38	6.70–10.97	<0.001
		120		12.02	7.76–13.54	
Kidney	40	60		13.71	12.14–15.32	<0.001
		120		16.20	13.95–19.45	
Blood pool	40	60		2.17	1.73–2.50	<0.001
		120		1.25	1.12–1.48	
Bone marrow	40	60		1.44	1.09–1.65	0.21
		120		1.38	0.99–1.72	
Urinary bladder	40	60		3.08	1.66–4.74	<0.001
		120		0.97	0.73–1.91	
Gluteus muscle	40	60		0.60	0.52–0.69	<0.001
		120		0.47	0.40–0.54	

[a] Wilcoxon's signed-ranks test

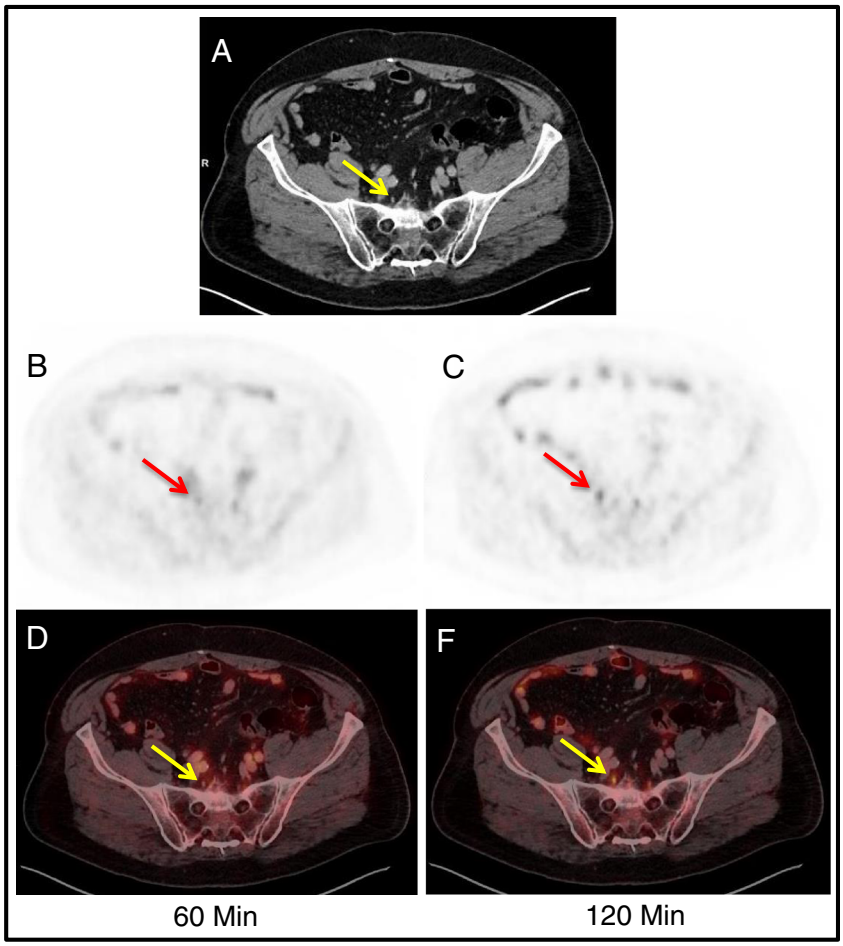

Fig. 2 Axial PET/CT images in a patient with biochemical relapse (PSA value 0.14 ng/ml) at 60 min (**b** PET image, **d** fused PET/CT image) and 120 min (**a** CT image, **c** PET image, **f** fused PET/CT) after injection. A lymph node with a diameter of 2 mm is differentiated by CT only on the late image (**a**). Uptake in the lymph node was differentiated retrospectively on the PET and fused PET/CT images at 60 min (**b**, **d**).

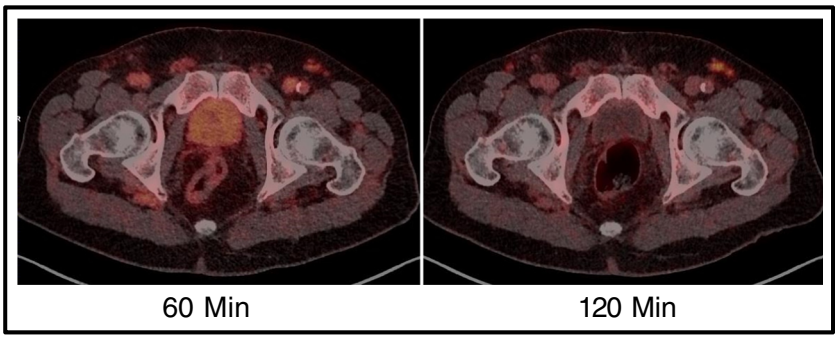

Fig. 3 Axial fused ^{18}F-PSMA-1007-PET/CT images showing early eliminated activity in the urinary bladder at 60 min after injection and nearly no activity in the urinary bladder at 120 min after injection.

activity could be detected in the ureter. At least in the time window used in the present study, ^{18}F-PSMA-1007 therefore showed an advantage over other PSMA ligands which are primarily eliminated via the kidneys [18]. At later time points, ^{18}F-PSMA-1007 is excreted via the urinary bladder [19].

Uptake in the bone/bone marrow remained stable. To the best of our knowledge PSMA has not been shown to be overexpressed in this compartment and the low uptake is probably nonspecific. In other organs, ^{18}F-PSMA-1007 uptake increased significantly: hepatic tracer elimination has been reported leading to considerable liver uptake of PSMA-1007. The range of SUV_{mean} in the liver showed a broad overlap with SUV_{max} in PCa lesions. This may lead to decreased sensitivity in the detection of liver metastasis, especially at 120 min after injection. An increase in tracer uptake in the kidneys has also been observed for PSMA-11 and PSMA-617 [5, 17]. Currently, we consider that this observation as well as increased uptake in the spleen is not relevant for clinical routine as metastases close to or within these organs are rare. Lesions characteristic of PCa showed significantly higher uptake and contrast in late images. The increasing uptake of PSMA ligands over time is an advantage of late acquisition which has been demonstrated in previous studies [5, 17, 20–22]. The results of the present analysis are therefore in accordance with the current literature.

All except one lesion were visible in images at 60 min after injection. However, it can be assumed that in larger patient cohorts, more lesions will be missed on early imaging. In accordance with the increasing uptake of PCa lesions over time as well as with the findings of the above-mentioned studies of different groups, we recommend that ^{18}F-PSMA-1007 PET/CT be performed at 120 min instead of 60 min after injection. The optimal time point for image acquisition using PSMA-1007 has not yet been evaluated. The current literature and our own experience suggest that the pharmacokinetics of ^{18}F-PSMA-1007 are slower than those of PSMA-11, which underlines the recommendation for a late scan. A head-to-head comparison of ^{18}F-PSMA-1007 and ^{68}Ga-PSMA-11 would be of great interest, but is not yet available.

The low urinary activity and the high tumour activity suggest that ^{18}F-PSMA-1007 has high potential for the detection of PCa especially in planning salvage radiotherapy in patients with biochemical relapse and low PSA values. This method may not only be helpful in excluding metastases outside the prostate bed but also guide dose painting to optimize efficacy of therapy.

One limitation of the present evaluation is the lack of histopathology. Therefore, we cannot exclude false-positive lesions. Although uptake of PSMA ligands in various nonprostatic tissues has been reported [6, 7], it has to be emphasized that the number of lesions detected in nonprostatic tissues represents only a small fraction of all PCa lesions detected by PSMA ligand imaging in clinical routine.

Conclusion

The uptake of ^{18}F-PSMA-1007 in PCa lesions shows a significant increase at 120 min compared with 60 min after injection. In addition, accumulation of the tracer in the urinary bladder is low and decreases over time, leading to improved contrast of adjacent PCa lesions. Increasing accumulation in the liver may limit the sensitivity of the tracer in detecting liver metastases. Larger studies are needed to evaluate the diagnostic performance of this new agent in detecting PCa.

Acknowledgments We thank the Radiochemistry Group at the Department of Nuclear Medicine for their highly reliable production of ^{18}F-PSMA-1007, as well as the technologists for their support.

Compliance with ethical standards

Disclosure The University of Münster received consulting fees from ABX GmbH, Radeberg, Germany for K.R. and M.B. Additionally K.R. is scientific consultant/advisor of ABX GmbH. The authors declare they have no conflict of interest according to the subject and matter of the present article.

Ethical approval All procedures performed in studies involving human participants were in accordance with the ethical standards of the institutional and/or national research committee and with the principles of the 1964 Declaration of Helsinki and its later amendments or comparable ethical standards. This article does not describe any studies with animals performed by any of the authors. According to data protection guidelines, formal ethical approval for retrospective studies is not necessary.

References

1. Siegel RL, Miller KD, Jemal A. Cancer statistics, 2015. CA Cancer J Clin. 2015;65(1):5–29. https://doi.org/10.3322/caac.21254.
2. Israeli RS, Powell CT, Corr JG, Fair WR, Heston WD. Expression of the prostate-specific membrane antigen. Cancer Res. 1994;54(7):1807–11.
3. Sweat SD, Pacelli A, Murphy GP, Bostwick DG. Prostate-specific membrane antigen expression is greatest in prostate adenocarcinoma and lymph node metastases. Urology. 1998;52(4):637–40.
4. Wright GL Jr, Grob BM, Haley C, Grossman K, Newhall K, Petrylak D, et al. Upregulation of prostate-specific membrane antigen after androgen-deprivation therapy. Urology. 1996;48(2):326–34.
5. Afshar-Oromieh A, Malcher A, Eder M, Eisenhut M, Linhart HG, Hadaschik BA, et al. PET imaging with a [68Ga]gallium-labelled PSMA ligand for the diagnosis of prostate cancer: biodistribution in humans and first evaluation of tumour lesions. Eur J Nucl Med Mol Imaging. 2013;40(4):486–95. https://doi.org/10.1007/s00259-012-2298-2.
6. Sheikhbahaei S, Afshar-Oromieh A, Eiber M, Solnes LB, Javadi MS, Ross AE, et al. Pearls and pitfalls in clinical interpretation of prostate-specific membrane antigen (PSMA)-targeted PET imaging. Eur J Nucl Med Mol Imaging. 2017;44(12):2117–36. https://doi.org/10.1007/s00259-017-3780-7.
7. Backhaus P, Noto B, Avramovic N, Grubert LS, Huss S, Bogemann M, et al. Targeting PSMA by radioligands in non-prostate disease-current status and future perspectives. Eur J Nucl Med Mol Imaging. 2018. https://doi.org/10.1007/s00259-017-3922-y.
8. Afshar-Oromieh A, Holland-Letz T, Giesel FL, Kratochwil C, Mier W, Haufe S, et al. Diagnostic performance of 68Ga-PSMA-11 (HBED-CC) PET/CT in patients with recurrent prostate cancer: evaluation in 1007 patients. Eur J Nucl Med Mol Imaging. 2017;44(8):1258–68. https://doi.org/10.1007/s00259-017-3711-7.
9. Afshar-Oromieh A, Avtzi E, Giesel FL, Holland-Letz T, Linhart HG, Eder M, et al. The diagnostic value of PET/CT imaging with the (68)Ga-labelled PSMA ligand HBED-CC in the diagnosis of recurrent prostate cancer. Eur J Nucl Med Mol Imaging. 2015;42(2):197–209. https://doi.org/10.1007/s00259-014-2949-6.
10. Eiber M, Maurer T, Souvatzoglou M, Beer AJ, Ruffani A, Haller B, et al. Evaluation of hybrid 68Ga-PSMA ligand PET/CT in 248 patients with biochemical recurrence after radical prostatectomy. J Nucl Med. 2015;56(5):668–74. https://doi.org/10.2967/jnumed.115.154153.
11. Rahbar K, Weckesser M, Huss S, Semjonow A, Breyholz HJ, Schrader AJ, et al. Correlation of intraprostatic tumor extent with 68Ga-PSMA distribution in patients with prostate cancer. J Nucl Med. 2016;57(4):563–7. https://doi.org/10.2967/jnumed.115.169243.
12. Afshar-Oromieh A, Zechmann CM, Malcher A, Eder M, Eisenhut M, Linhart HG, et al. Comparison of PET imaging with a (68)Ga-labelled PSMA ligand and (18)F-choline-based PET/CT for the diagnosis of recurrent prostate cancer. Eur J Nucl Med Mol Imaging. 2014;41(1):11–20. https://doi.org/10.1007/s00259-013-2525-5.
13. Mease RC, Dusich CL, Foss CA, Ravert HT, Dannals RF, Seidel J, et al. N-[N-[(S)-1,3-Dicarboxypropyl]carbamoyl]-4-[18F]fluorobenzyl-L-cysteine, [18F]DCFBC: a new imaging probe for prostate cancer. Clin Cancer Res. 2008;14(10):3036–43. https://doi.org/10.1158/1078-0432.CCR-07-1517.
14. Szabo Z, Mena E, Rowe SP, Plyku D, Nidal R, Eisenberger MA, et al. Initial evaluation of [(18)F]DCFPyL for prostate-specific membrane antigen (PSMA)-targeted PET imaging of prostate cancer. Mol Imaging Biol. 2015;17(4):565–74. https://doi.org/10.1007/s11307-015-0850-8.
15. Giesel FL, Kesch C, Yun M, Cardinale J, Haberkorn U, Kopka K, et al. 18F-PSMA-1007 PET/CT detects micrometastases in a patient with biochemically recurrent prostate cancer. Clin Genitourin Cancer. 2017;15(3):e497–9. https://doi.org/10.1016/j.clgc.2016.12.029.
16. Cardinale J, Schafer M, Benesova M, Bauder-Wust U, Leotta K, Eder M, et al. Preclinical evaluation of 18F-PSMA-1007, a new prostate-specific membrane antigen ligand for prostate cancer imaging. J Nucl Med. 2017;58(3):425–31. https://doi.org/10.2967/jnumed.116.181768.
17. Afshar-Oromieh A, Hetzheim H, Kratochwil C, Benesova M, Eder M, Neels OC, et al. The theranostic PSMA ligand PSMA-617 in the diagnosis of prostate cancer by PET/CT: biodistribution in humans, radiation dosimetry, and first evaluation of tumor lesions. J Nucl Med. 2015;56(11):1697–705. https://doi.org/10.2967/jnumed.115.161299.
18. Rahbar K, Weckesser M, Ahmadzadehfar H, Schafers M, Stegger L, Bogemann M. Advantage of (18)F-PSMA-1007 over (68)Ga-PSMA-11 PET imaging for differentiation of local recurrence vs. urinary tracer excretion. Eur J Nucl Med Mol Imaging. 2018; https://doi.org/10.1007/s00259-018-3952-0.
19. Giesel FL, Hadaschik B, Cardinale J, Radtke J, Vinsensia M, Lehnert W, et al. F-18 labelled PSMA-1007: biodistribution, radiation dosimetry and histopathological validation of tumor lesions in prostate cancer patients. Eur J Nucl Med Mol Imaging. 2017;44(4):678–88. https://doi.org/10.1007/s00259-016-3573-4.
20. Afshar-Oromieh A, Hetzheim H, Kubler W, Kratochwil C, Giesel FL, Hope TA, et al. Radiation dosimetry of (68)Ga-PSMA-11 (HBED-CC) and preliminary evaluation of optimal imaging timing. Eur J Nucl Med Mol Imaging. 2016;43(9):1611–20. https://doi.org/10.1007/s00259-016-3419-0.
21. Afshar-Oromieh A, Sattler LP, Mier W, Hadaschik BA, Debus J, Holland-Letz T, et al. The clinical impact of additional late PET/CT imaging with 68Ga-PSMA-11 (HBED-CC) in the diagnosis of prostate cancer. J Nucl Med. 2017;58(5):750–5. https://doi.org/10.2967/jnumed.116.183483.
22. Herrmann K, Bluemel C, Weineisen M, Schottelius M, Wester HJ, Czernin J, et al. Biodistribution and radiation dosimetry for a probe targeting prostate-specific membrane antigen for imaging and therapy. J Nucl Med. 2015;56(6):855–61. https://doi.org/10.2967/jnumed.115.156133.